Supporting Information

Multifunctional Fluorescent Copper Nanoclusters for Ag^+ Sensing, Anti-counterfeiting and Blue/White Light-emitting Diodes

Cheng Zhang[a], Congying Shao[a]*, Junsheng Wang[a], Ziwei Li[a], Mengna Liang[a], Yongxiang Wang[a], Dan Liu[b], Shun Lu[c]*

a Key Laboratory of Green and Precise Synthetic Chemistry, Ministry of Education, College of Chemistry and Materials Science, Huaibei Normal University, Huaibei, Anhui 235000, China

b School of Chemistry and Chemical Engineering, Chongqing University,174 Shazheng Street, Shapingba District, Chongqing, 400044, China

c Chongqing Institute of Green and Intelligent Technology, Chinese Academy of Sciences, Chongqing, 400714, China

* Emails: shaocongying@163.com (CY. Shao), and lushun@cigit.ac.cn (S. Lu)

Figures: 7
Tables: 2

Table S1 Comparison of fluorescence methods for Ag^+ detection

Type of probe	Detection range	LOD（nM）	Ref
Aperylene derivative	0 ~ 100 μM	50	[1]
G-CDs	0 ~ 80 μM	90	[2]
UCNPs	0 ~ 0.5 mM	33	[3]
Tri-HC_3N_4	1 ~ 100 μM	404.6	[4]
Ti_3C_2 NSs	0.1 ~ 40 μM	9.7	[5]
C_{SM}-Dots	5 ~ 290 μM	500	[6]
N-H-CQDs	0 ~ 100 μM	242	[7]
DPA@Ag NCs	0.05 ~ 800 μM	30	[8]
MMI-CuNCs	0.025 ~ 50 μM	6.7	This work

Table S2 Comparison of fluorescence quantum yields (QYs) of different blue emissive CuNCs

Type of CuNCs	QYs	Ref
Pespsin-CuNCs	13.61%	[9]
GSH-CuNCs	8.6%	[10]
CuNCs@TA	9.8%	[11]
Lysozyme-CuNCs	18%	[12]
CuNCs@Tryp	3.6%	[13]
BSA-CuNCs	3.47%	[14]
CuNCs@Trp	3.01%	[15]
CuNCs-CA	2.3%	[16]
CuNCs@FA	19.1%	[17]
MMI-CuNCs	19.2%	This work

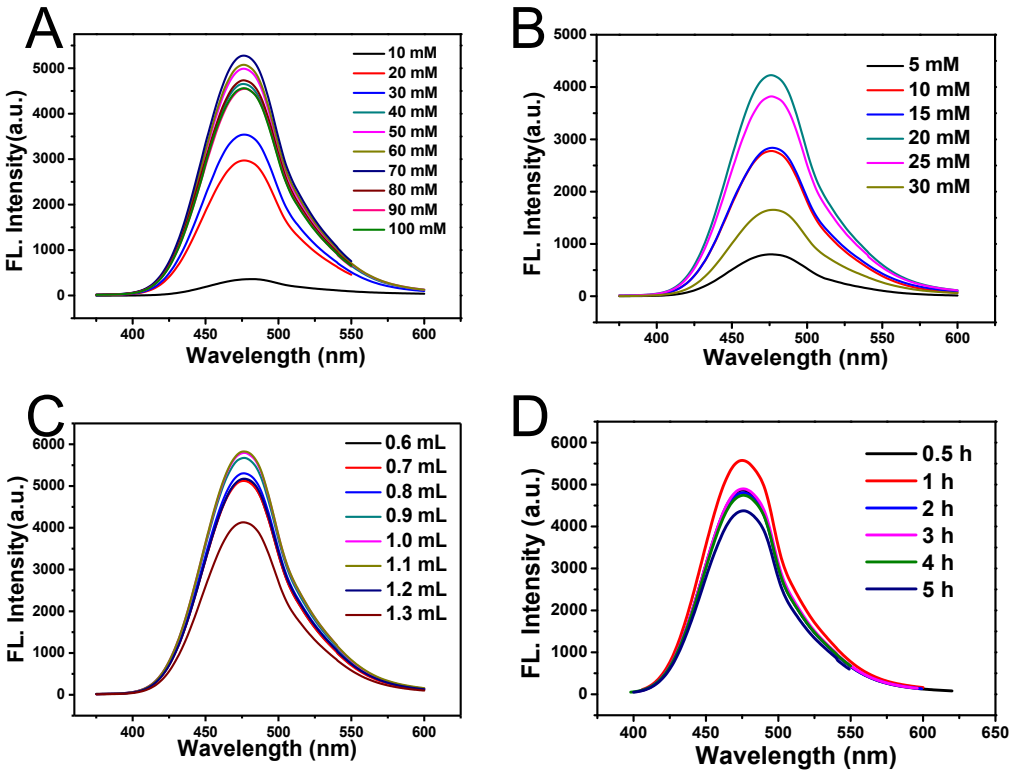

Figure S1. Effects of concentration of $CuSO_4$ (A), concentration of MMI (B), volume of hydrazine hydrate (C) and reaction time (D) on fluorescence properties of MMI-CuNCs.

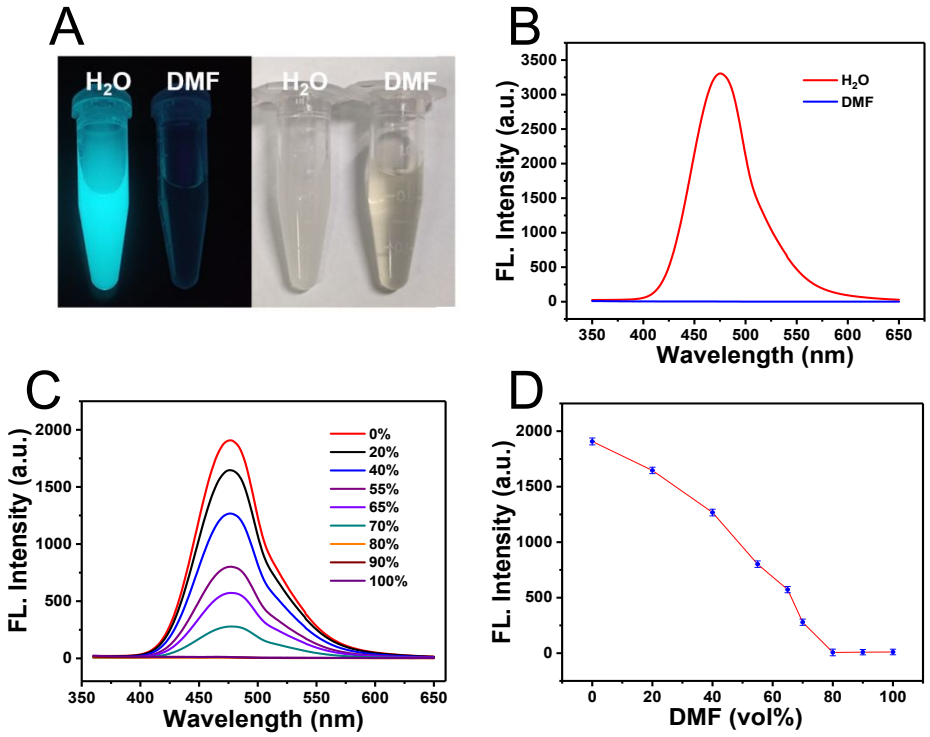

Figure S2. (A) Images of MMI-CuNCs dispersed in water and DMF under 365 nm UV lamp (left) and sunlight (right). (B) FL emission spectra of MMI-CuNCs dispersed in water and DMF, respectively. (C) FL emission spectra of MMI-CuNCs dispersed in the water/DMF mixtures with different volumetric fractions of DMF (vol%). (D) Pot of fluorescence intensity of MMI-CuNCs versus the volumetric fractions of DMF.

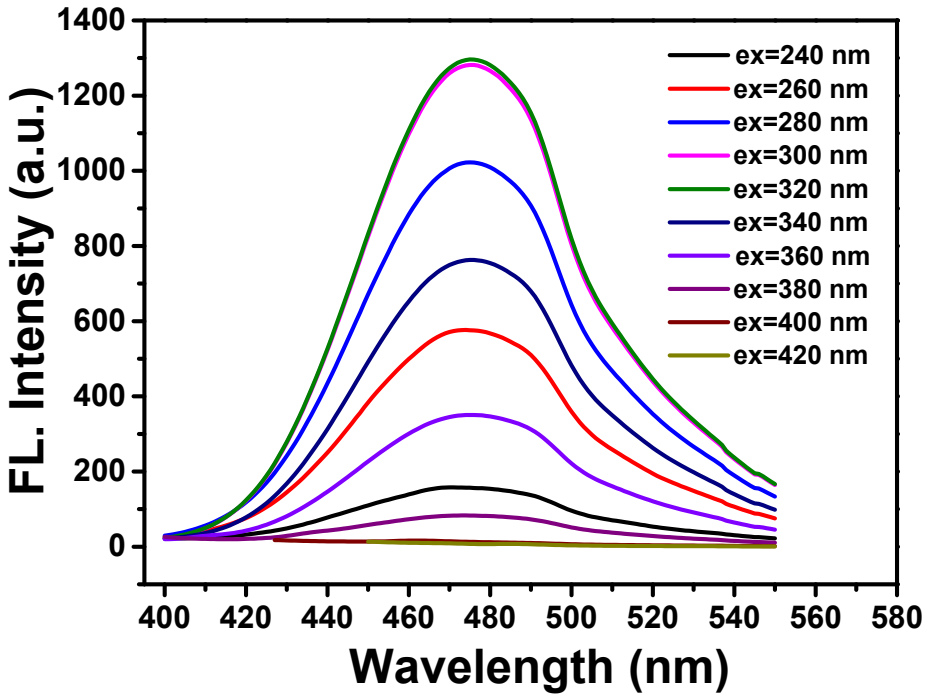

Figure S3. Emission spectra of MMI-CuNCs dispersed in ethanol at different excitation wavelengths progressively increasing from 240 to 420 nm.

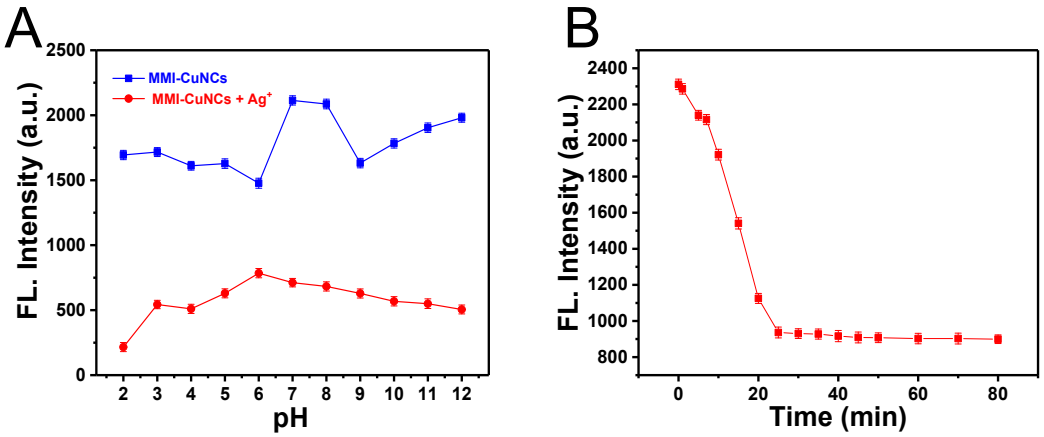

Figure S4. Optimization of detection conditions. (A) Effect of the solution pH values. (B) Effect of the incubation time.

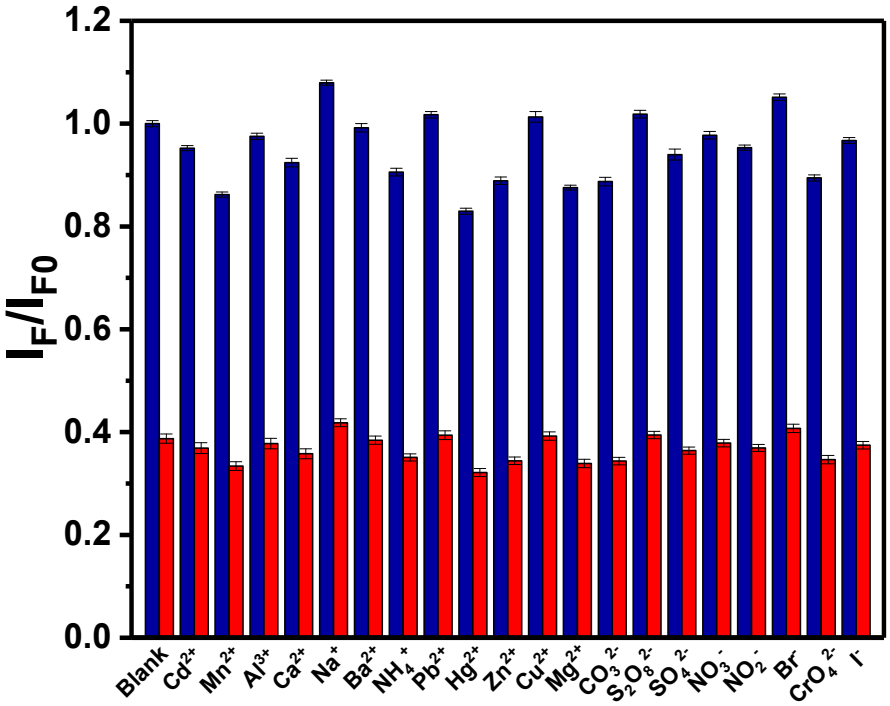

Figure S5. Selectivity of MMI-CuNCs toward different ions in the absence (blue column) and presence (red column) of Ag^{+}.

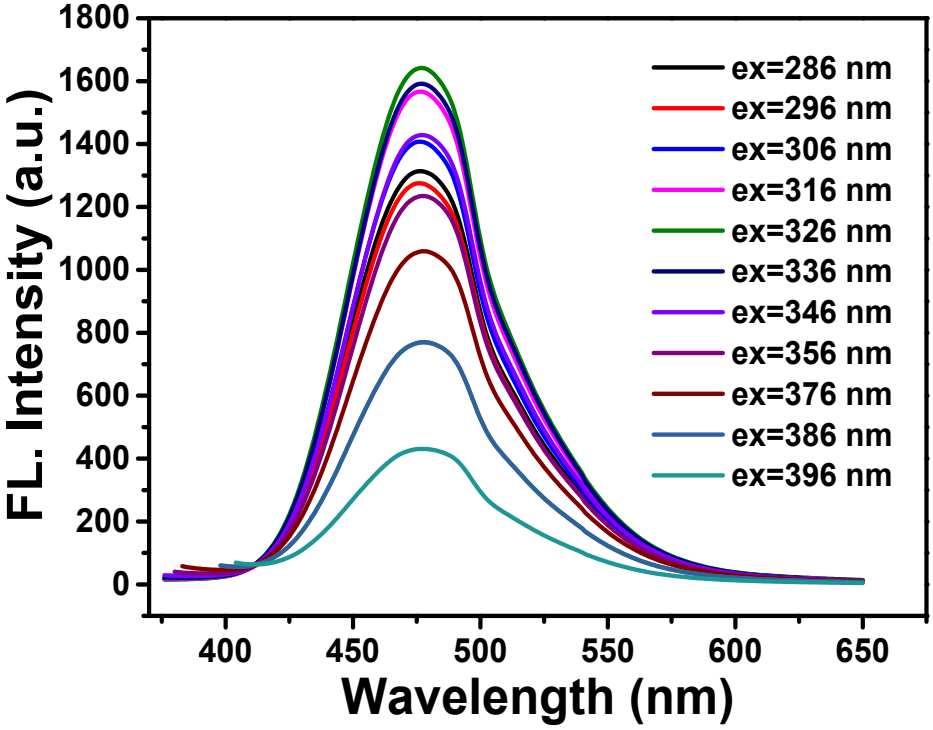

Figure. S6 Emission spectra of solid phase MMI-CuNCs at different excitation wavelengths progressively increasing from 286 to 396 nm.

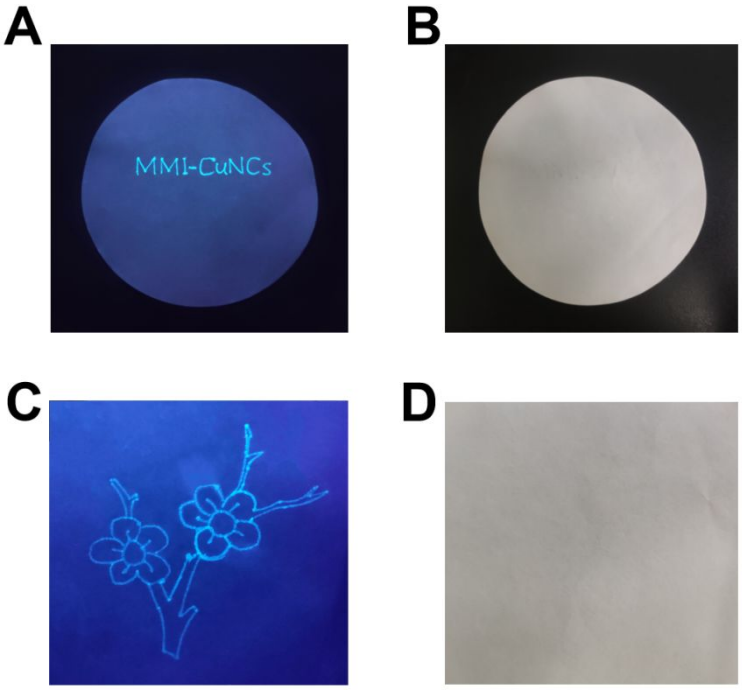

Figure S7. Long-term stability of the luminescence images drawn by MMI-CuNCs ink. The photos were taken under a 365 nm UV lamp (A and C) and sunlight (B and D) after nine months kept in atmosphere environment.

References

(1) Lu, Y.; Meng, L.; Gao, Y.; Liao, D.; Li, Y.; Ai, Y.; Ma, Y.; Yu, C. A label free Ag^+ sensing method via in situ formation of metal coordination polymer. *Anal. Biochem.* **2018**, *549*, 21-25.

(2) Li, Q.; Bai, Z.; Xi, X.; Guo, Z.; Liu, C.; Liu, X.; Zhao, X.; Li, Z.; Cheng, Y.; Wei, Y. Rapid microwave-assisted green synthesis of guanine-derived carbon dots for highly selective detection of Ag^+ in aqueous solution. *Spectrochim. Acta A Mol. Biomol. Spectrosc.* **2021**, *248*, 119208.

(3) Long, Q.; Wen, Y.; Li, H.; Zhang, Y.; Yao, S. A novel fluorescent biosensor for detection of silver ions based on upconversion nanoparticles. *J. Fluoresc.* **2017**, *27*, 205-211.

(4) Hao, L.; Song, H.; Lv, Y. Modified triazine-based carbon nitride as a high efficiency fluorescence sensor for the label-free detection of Ag^+. *J. Mater. Res.* **2020**, *35*, 3235-3246.

(5) Desai, M. L.; Basu, H.; Singhal, R. K.; Saha, S.; Kailasa, S. K. Ultra-small two dimensional MXene nanosheets for selective and sensitive fluorescence detection of Ag^+ and Mn^{2+} ions. *Colloid. Surface. A* **2019**, *565*, 70-77.

(6) Zhou, X.; Cao, Y.; Zhou, X.; Xu, L.; Zhang, D.; Wang, C.; Chu, F.; Qian, T. Nanosensors based on structural memory carbon nanodots for Ag^+ fluorescence determination. *Nanomaterials* **2021**, *11*, 2687.

(7) Jiang, X.; Huang, J.; Chen, T.; Zhao, Q.; Xu, F.; Zhang, X. Synthesis of hemicellulose/deep eutectic solvent based carbon quantum dots for ultrasensitive detection of Ag^+ and L-cysteine with "off-on" pattern. *Int. J. Biol. Macromol.* **2020**, *153*, 412-420.

(8) An, M.; Li, H.; Su, M.; Gao, S.; Wang, M. C.; Shen, S. G.; Gao, Z. F.; Dong, J. X. Cu^{2+} enhanced fluorescent Ag nanoclusters with tunable emission from red to yellow and the application for Ag^+ sensing. *Spectrochim. Acta A Mol. Biomol. Spectrosc.* **2021**, *252*, 119484.

(9) Borse, S.; Murthy, Z.; Park, T.-J.; Kailasa, S. K. Pepsin mediated synthesis of blue fluorescent copper nanoclusters for sensing of flutamide and chloramphenicol drugs. *Microchem. J.* **2021**, *164*, 105947.

(10) Huang, H.; Li, H.; Feng, J.-J.; Feng, H.; Wang, A.-J.; Qian, Z. One-pot green synthesis of highly fluorescent glutathione-stabilized copper nanoclusters for Fe^{3+} sensing. *Sens. Actuators B Chem.* **2017**, *241*, 292-297.

(11) Guo, Y.-y.; Hu, Y.-r.; Chen, S.-k.; Guo, M.-z.; Zhang, Y.-t.; Han, X.-r.; Zhang, S. Facile one-pot synthesis of tannic acid-stabilized fluorescent copper nanoclusters and its application as sensing probes

for chlortetracycline based on inner filter effect. *Colloid. Surface. A* **2022**, *634*, 127962.

(12) Ghosh, R.; Sahoo, A. K.; Ghosh, S. S.; Paul, A.; Chattopadhyay, A. Blue-emitting copper nanoclusters synthesized in the presence of lysozyme as candidates for cell labeling. *ACS Appl. Mater. Interfaces* **2014**, *6*, 3822-3828.

(13) Guo, Y.-y.; Li, W.-j.; Guo, P.-y.; Han, X.-r.; Deng, Z.-r.; Zhang, S.; Cai, Z.-f. One facile fluorescence strategy for sensitive determination of baicalein using trypsin-templated copper nanoclusters. *Spectrochim. Acta A Mol. Biomol. Spectrosc.* **2022**, *268*, 120689.

(14) Fan, Y.; Yu, W.; Liao, Y.; Jiang, X.; Wang, Z.; Cheng, Z. Ratiometric detection of doxycycline in pharmaceutical based on dual ligands-enhanced copper nanoclusters. *Spectrochim. Acta A Mol. Biomol. Spectrosc.* **2022**, *267*, 120509.

(15) Kardar, Z. S.; Shemirani, F.; Zadmard, R. Determination of iron (II) and iron (III) via static quenching of the fluorescence of tryptophan-protected copper nanoclusters. *Microchim. Acta* **2020**, *187*, 1-9.

(16) Bao, Z.; Zhang, K.; Jian, J.; Hu, Z.; Yuan, K.; Shao, H.; Peng, K.; Jiang, Z.; Zapien, J. A.; Yan, Y. Strongly fluorescent cysteamine-coated copper nanoclusters as a fluorescent probe for determination of picric acid. *Microchim. Acta* **2018**, *185*, 1-7.

(17) Bai, Y.; Liu, J.; Feng, F.; Yang, X. Synthesis of folic acid-mediated copper nanoclusters for the detection of sulfadiazine sodium. *Colloid. Surface. A* **2020**, *605*, 125376.